

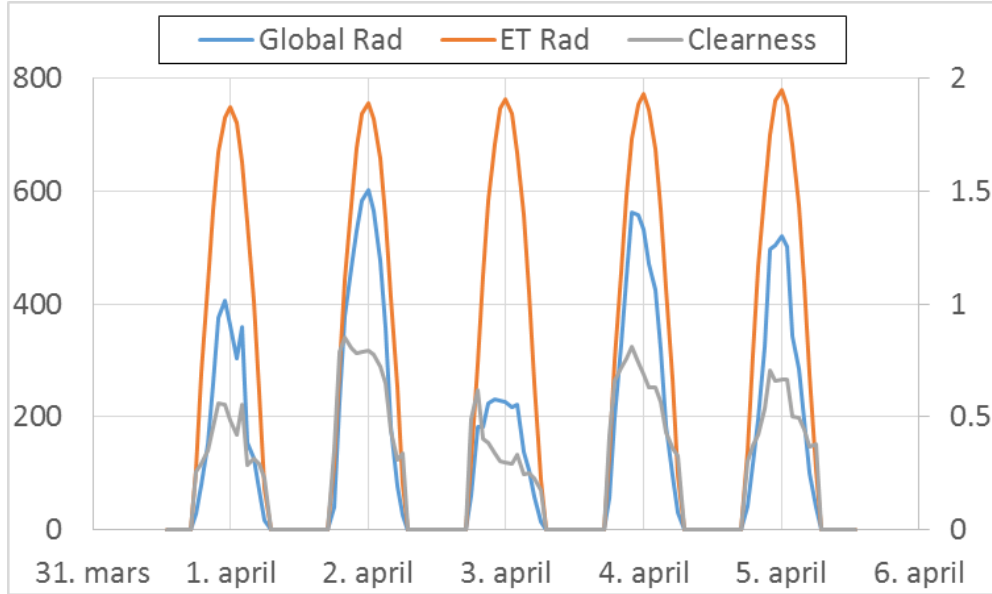
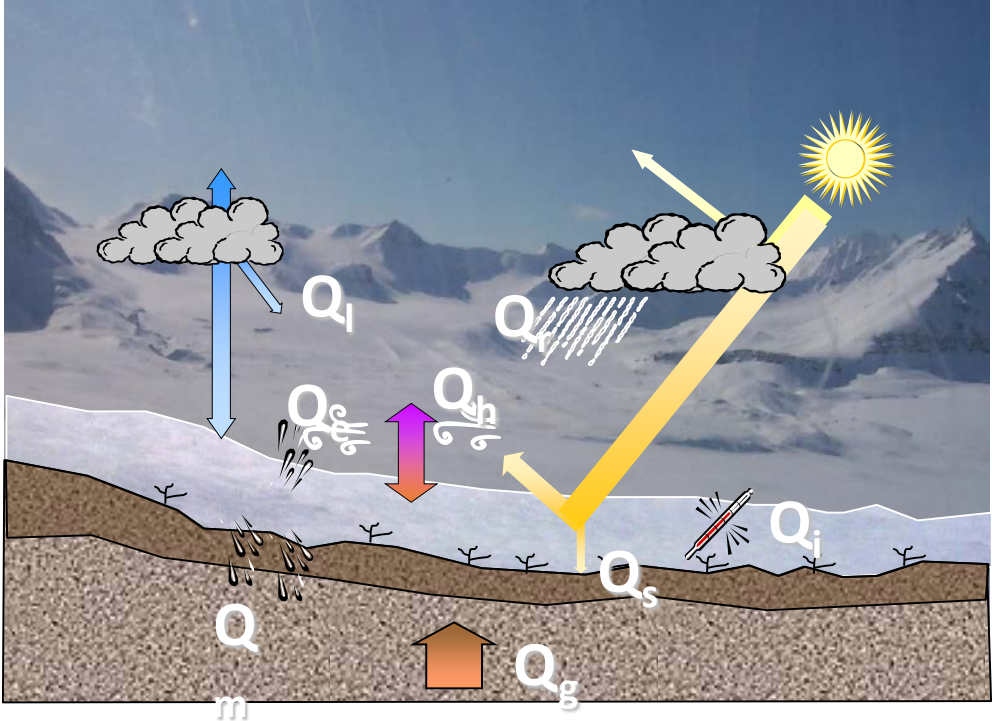
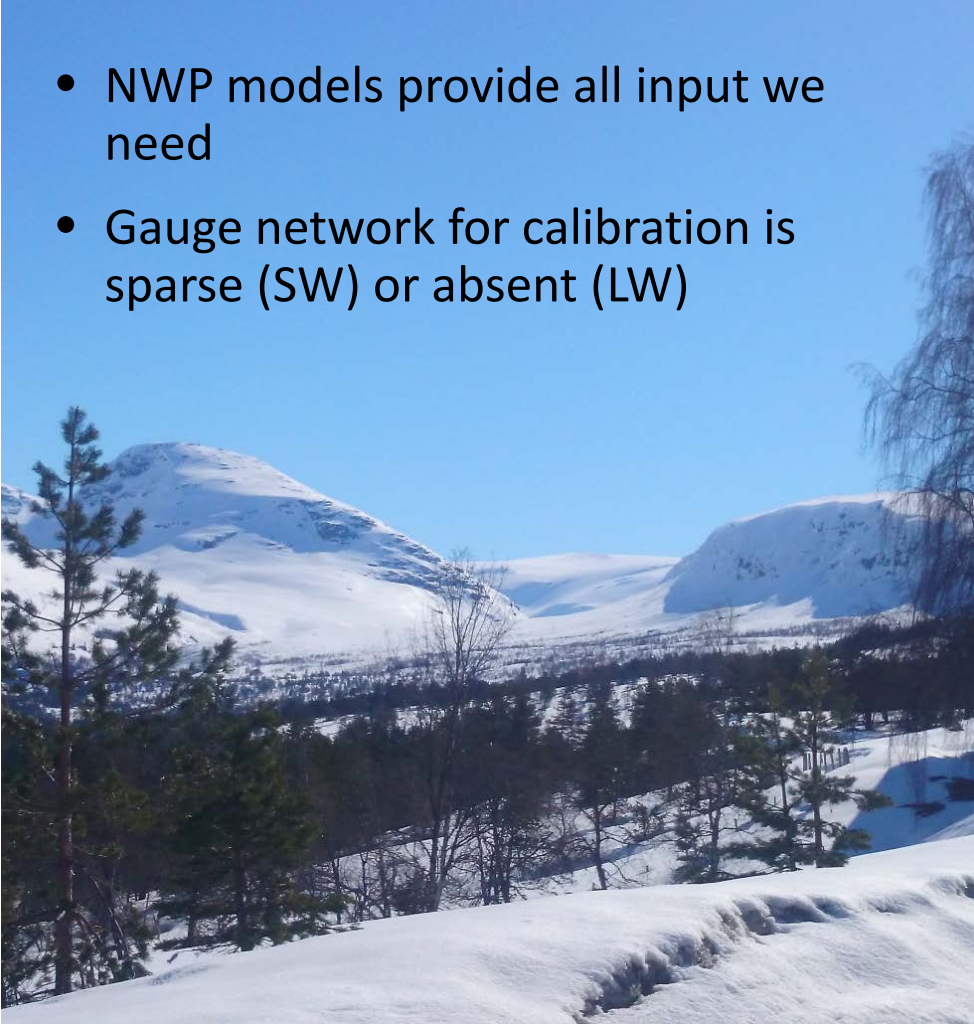
A satellite view of the Arctic region of Earth, showing the continent of Antarctica and surrounding ice sheets. The image displays a complex pattern of snowmelt, with dark green and black areas indicating melted snow and ice, and lighter green and white areas indicating remaining snow and ice. The text "High-frequency satellite radiation data in snowmelt modelling" is overlaid on the image in a semi-transparent grey box.

# High-frequency satellite radiation data in snowmelt modelling

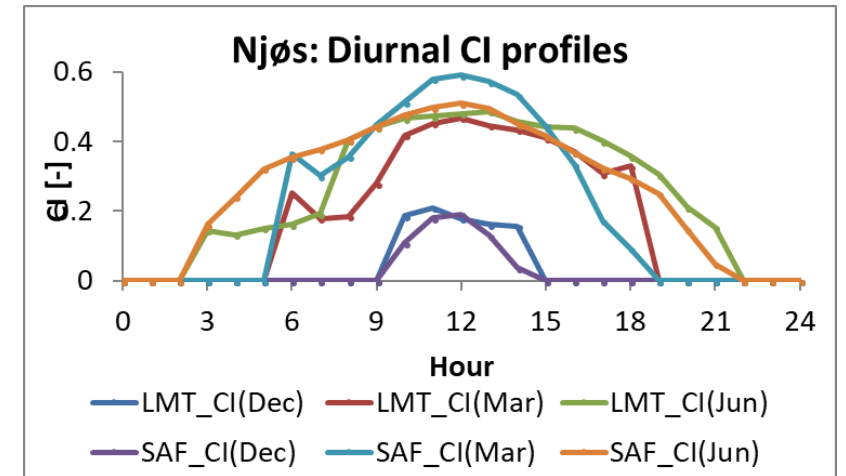
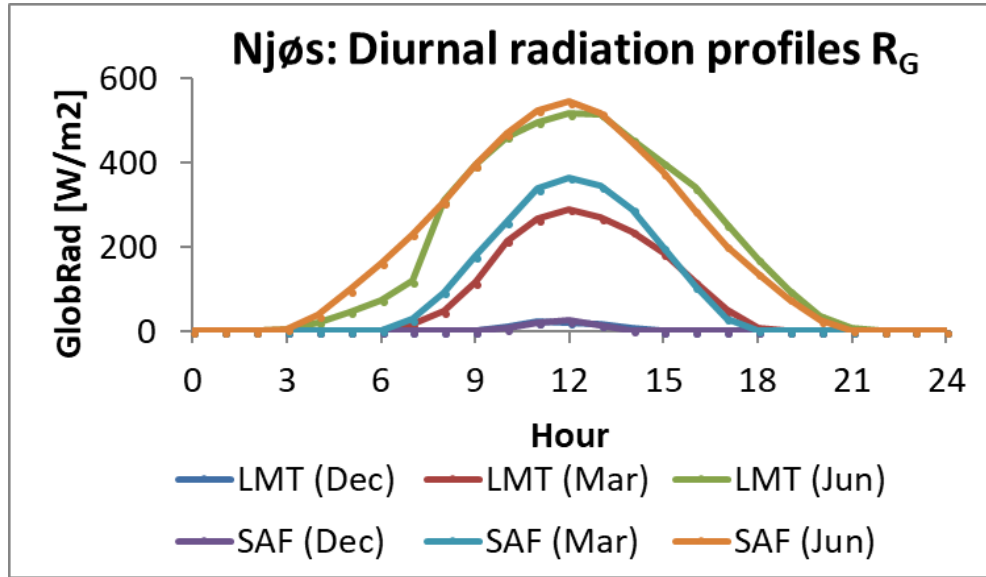
Sjur Kolberg, Enki hydrologi

# Energy budget of snow melt

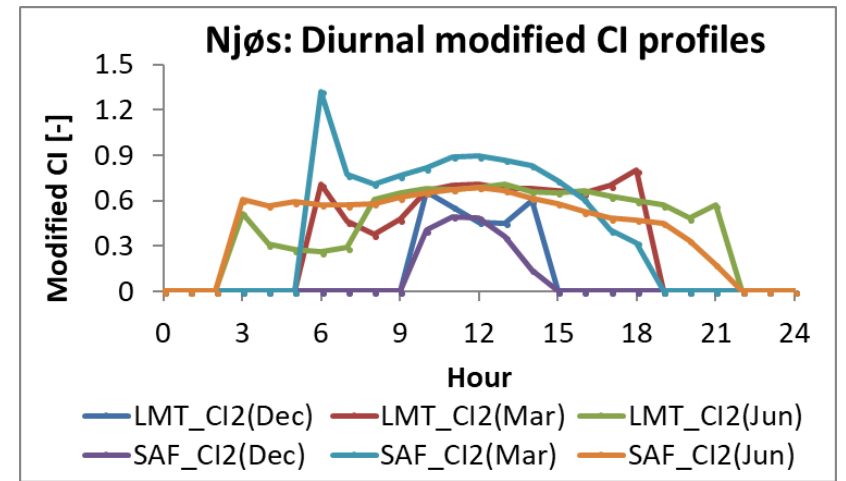
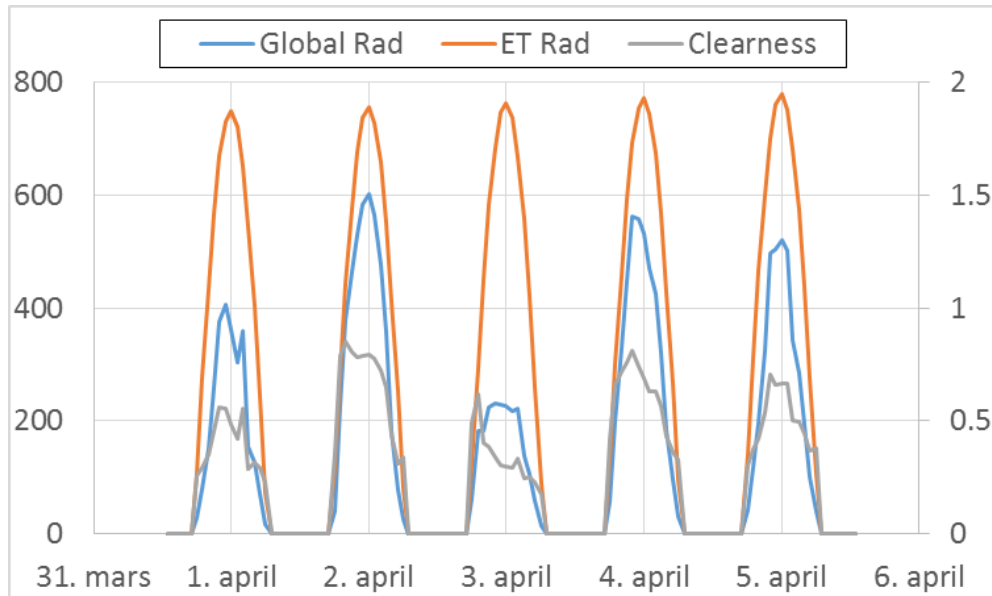
$$Q_s + Q_l + Q_h + Q_e + Q_g + Q_r = Q_i + Q_m$$



# Radiation and clearness indices

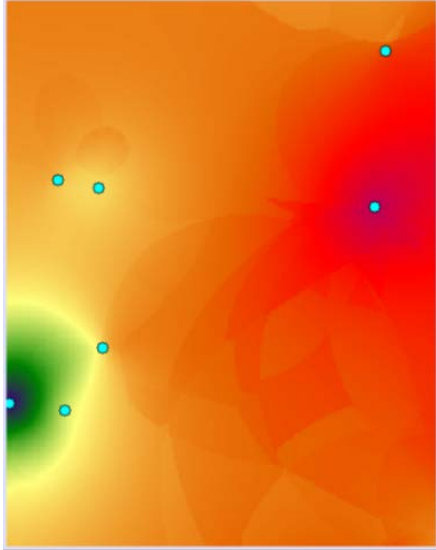


$$CI = \frac{R_G}{S_c \sin \alpha}$$

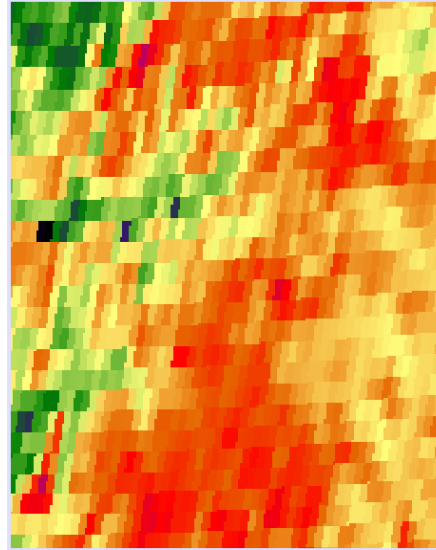


$$CI' = \frac{R_G}{S_c \sin \alpha} \cdot F(\tau_{atm})$$

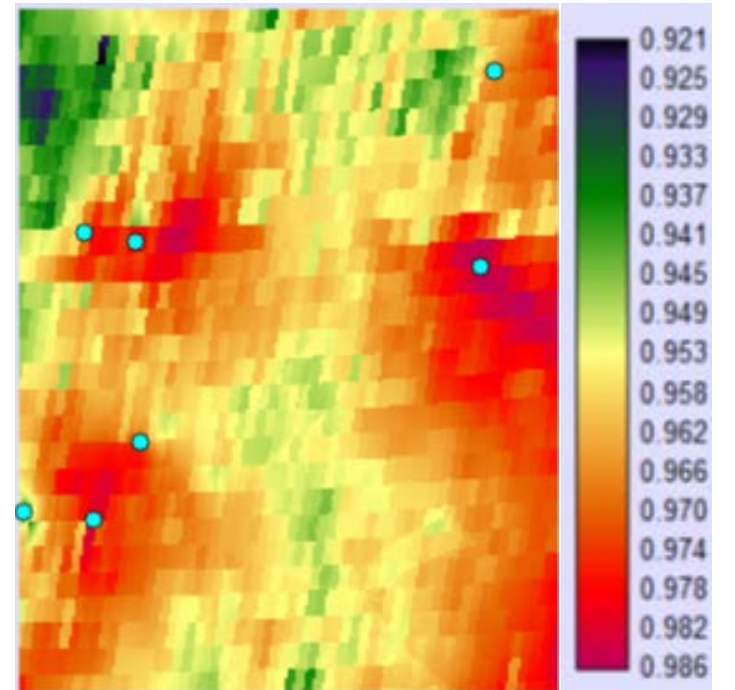
# SEVIRI SW data evaluation



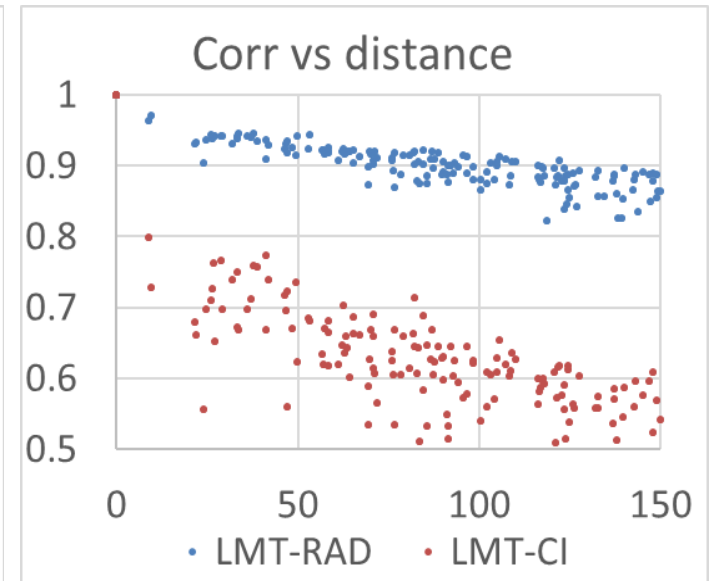
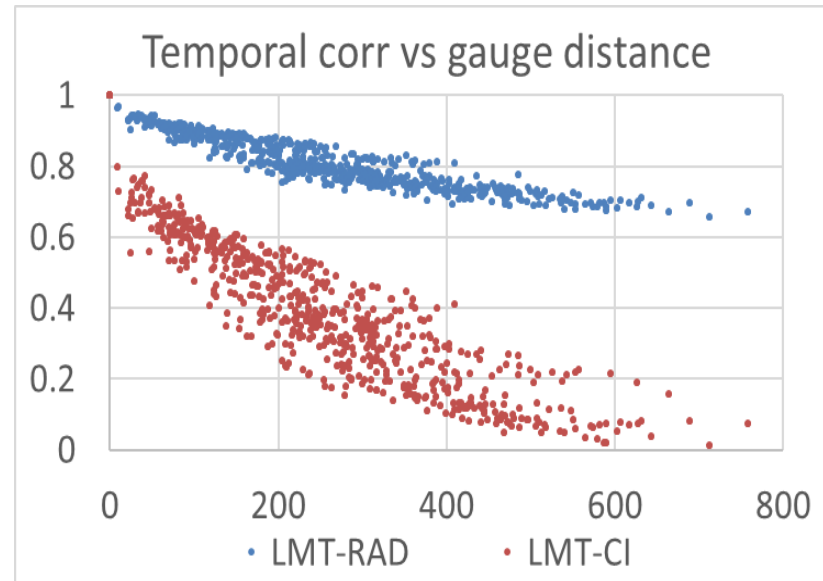
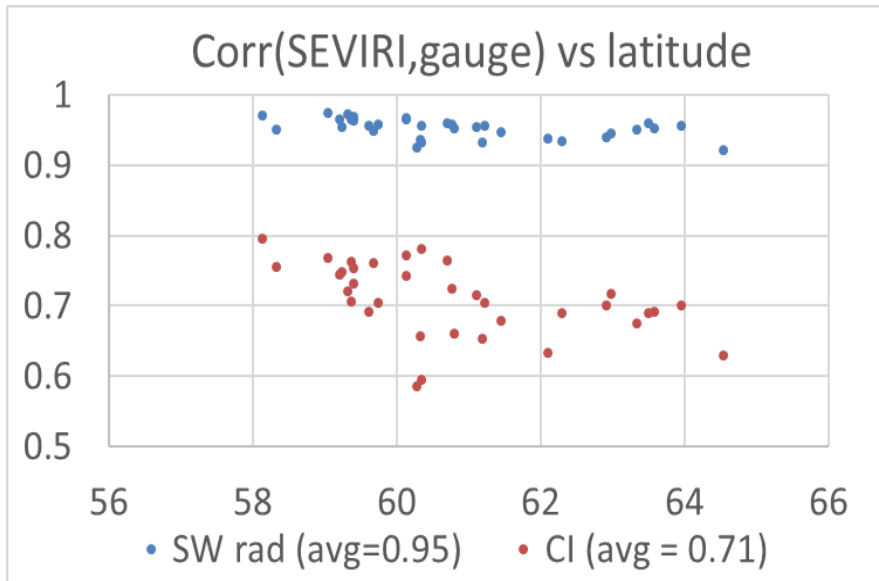
Interp. annual avg.



SEVIRI annual avg



Corr ( SEVIRI , interpolation )



# Longwave radiation

- No gauge network available, only a few project based series.

- Clear-sky radiation model:

$$SW_{CS}^{\downarrow} = \sigma \varepsilon_{sky} T_{sky}^4$$

- Clear-sky emissivity models

- Prata 1996):
- Brutsaert 1975:
- (and many more)

$$\varepsilon_{CS} = 1 - \left(1 + \frac{w}{10}\right) \cdot \exp\left(-\left(\alpha + \beta \frac{w}{10}\right)^m\right)$$

$$\varepsilon_{CS} = \alpha \cdot \left(\frac{P_w}{T_A}\right)^\beta$$

- Cloud correction

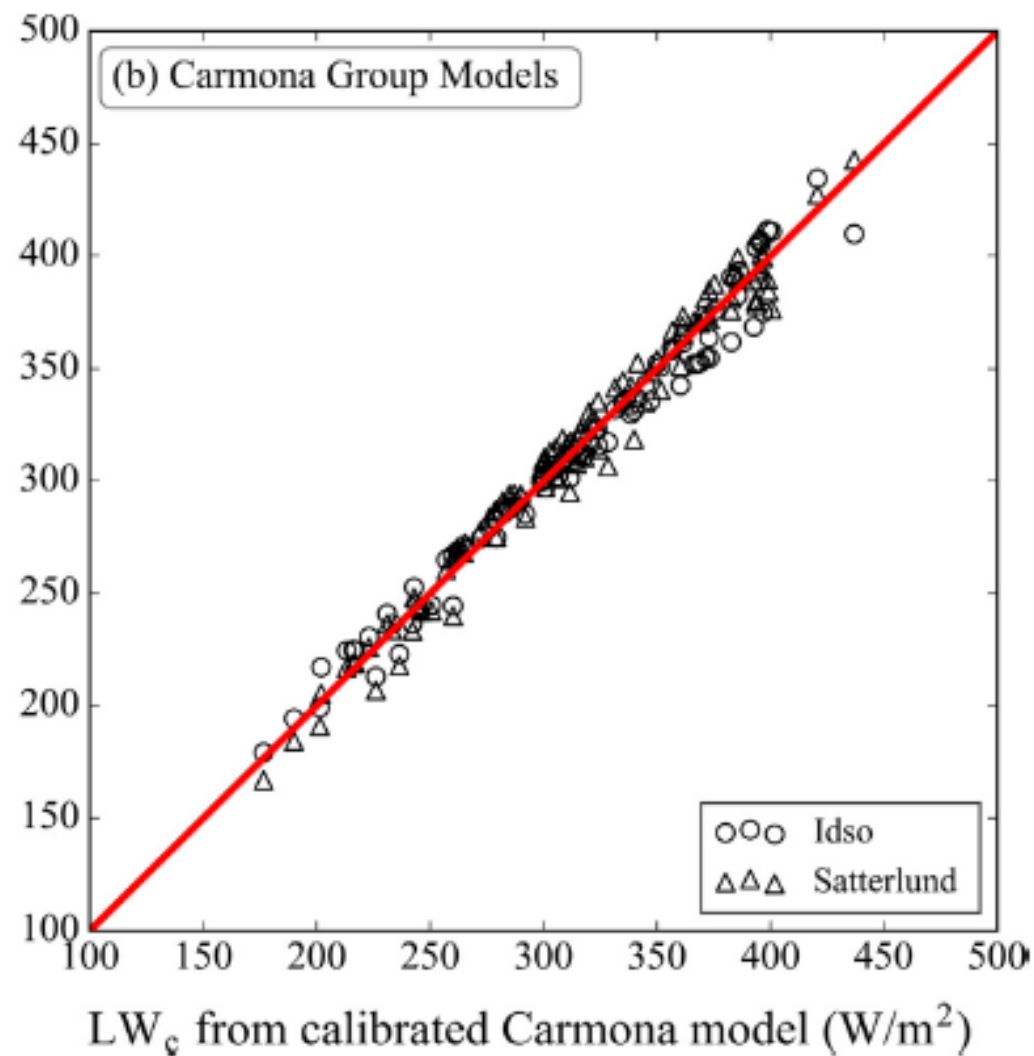
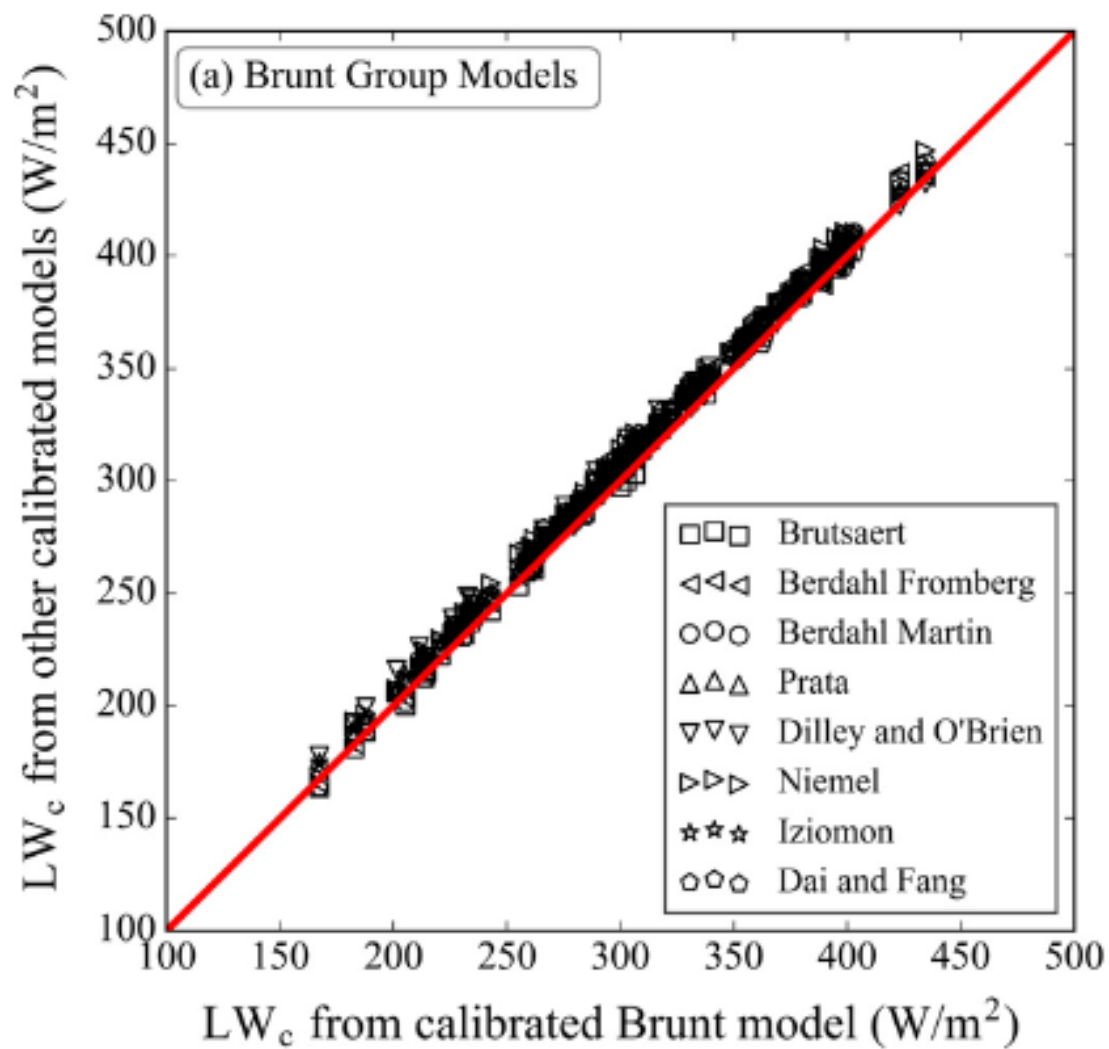
$$SW^{\downarrow} = n + (1 - n) \varepsilon_{CS}$$

# Models for clear-sky longwave radiation

Parametric models for clear skies.

Model	Year Developed	Variables	Formulation	Original Parameters
Brunt (1932)	1932	$P_w$ (hPa)	$\epsilon_{sky} = c_1 + c_2 \sqrt{P_w}$	$c_1 = 0.52, c_2 = 0.065$
Swinbank (1963)	1963	$T_a$ (K)	$\epsilon_{sky} = c_1 T_a^{c_2}$	$c_1 = 9.365 \times 10^{-6}, c_2 = 2$
Idso and Jackson (1969)	1969	$T_a$ (K)	$\epsilon_{sky} = 1 - c_1 \exp[c_2 (273 - T_a)^{c_3}]$	$c_1 = 0.261, c_2 = -7.77 \times 10^{-4}, c_3 = 2$
Brutsaert (1975)	1975	$P_w$ (hPa), $T_a$ (K)	$\epsilon_{sky} = c_1 (P_w/T_a)^{c_2}$	$c_1 = 1.24, c_2 = 1/7$
Satterlund (1979)	1979	$P_w$ (hPa), $T_a$ (K)	$\epsilon_{sky} = c_1 [1 - \exp(-P_w^{T_a/c_2})]$	$c_1 = 1.08, c_2 = 2016$
Idso (1981)	1981	$P_w$ (hPa), $T_a$ (K)	$\epsilon_{sky} = c_1 + c_2 P_w \exp(c_3/T_a)$	$c_1 = 0.70, c_2 = 5.95 \times 10^{-5}, c_3 = 1500$
Berdahl and Fromberg (1982)	1982	$T_d$ (°C)	$\epsilon_{sky} = c_1 + c_2 T_d$ (daytime)	$c_1 = 0.727, c_2 = 0.0060$
Berdahl and Martin (1984)	1984	$T_d$ (°C)	$\epsilon_{sky} = c_1 + c_2 (T_d/100) + c_3 (T_d/100)^2$	$c_1 = 0.711, c_2 = 0.56, c_3 = 0.73$
Prata (1996)	1996	$w$ (g/cm <sup>2</sup> ), $P_w$ (hPa), $T_a$ (K)	$\epsilon_{sky} = 1 - (1 + w) \exp(-\sqrt{(c_1 + c_2 w)}), w = c_3 \frac{P_w}{T_a}$	$c_1 = 1.2, c_2 = 3, c_3 = 46.5$
Dilley and O'Brien (1998)	1998	$T_a$ (K), $w$ (kg/m <sup>2</sup> )	$\epsilon_{sky} = \left( c_1 + c_2 \left( \frac{T_a}{273.15} \right)^6 + c_3 \sqrt{\frac{w}{25}} \right) / \sigma T_a^4, w = 4.65 \frac{P_w}{T_a}$	$c_1 = 59.38, c_2 = 113.7, c_3 = 96.96$
Niemelä et al. (2001)	2001	$P_w$ (hPa)	$\epsilon_{sky} = c_1 + c_2 (P_w - c_3), \text{ if } P_w \geq c_3$ $\epsilon_{sky} = c_1 - c_2 (P_w - c_3), \text{ if } P_w < c_3$	$c_1 = 0.72, c_2 = 0.009, c_3 = 2$ $c_1 = 0.72, c_2 = 0.076, c_3 = 2$
Iziomon et al. (2003)	2003	$P_w$ (hPa), $T_a$ (K)	$\epsilon_{sky} = 1 - c_1 \exp\left(\frac{-10P_w}{T_a}\right)$	$c_1 = 0.35$
Ruckstuhl et al. (1984)	2007	$w$ (mm), $d$ (g/kg)	$\epsilon_{sky} = c_1 w^{c_2}, w = c_3 d - c_4$	$c_1 = 147.8, c_2 = 0.26, c_3 = 2.40, c_4 = 1.60$
Dai and Fang (2014)	2014	$P_w$ (hPa), $P_a$ (hPa)	$\epsilon_{sky} = (c_1 + c_2 P_w^{c_3})(P_a/1013)^{c_4}$	$c_1 = 0.48, c_2 = 0.17, c_3 = 0.22, c_4 = 0.45$
Carmona et al. (2014)	2014	$T_a$ (K), $\phi$ (%)	$\epsilon_{sky} = -c_1 + c_2 T_a + c_3 \phi$	$c_1 = 0.34, c_2 = 3.36 \times 10^{-3}, c_3 = 1.94 \times 10^{-3}$

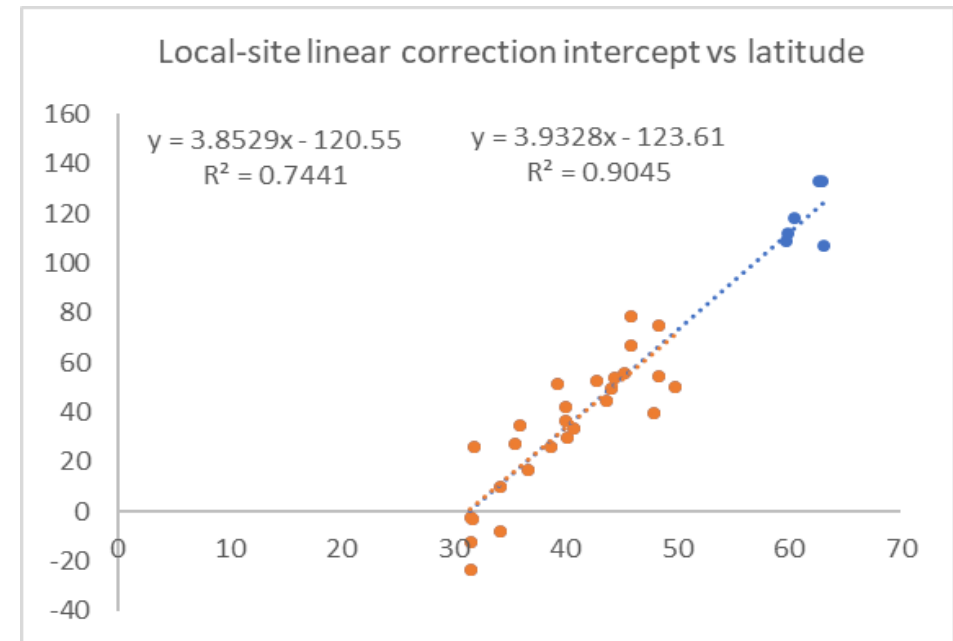
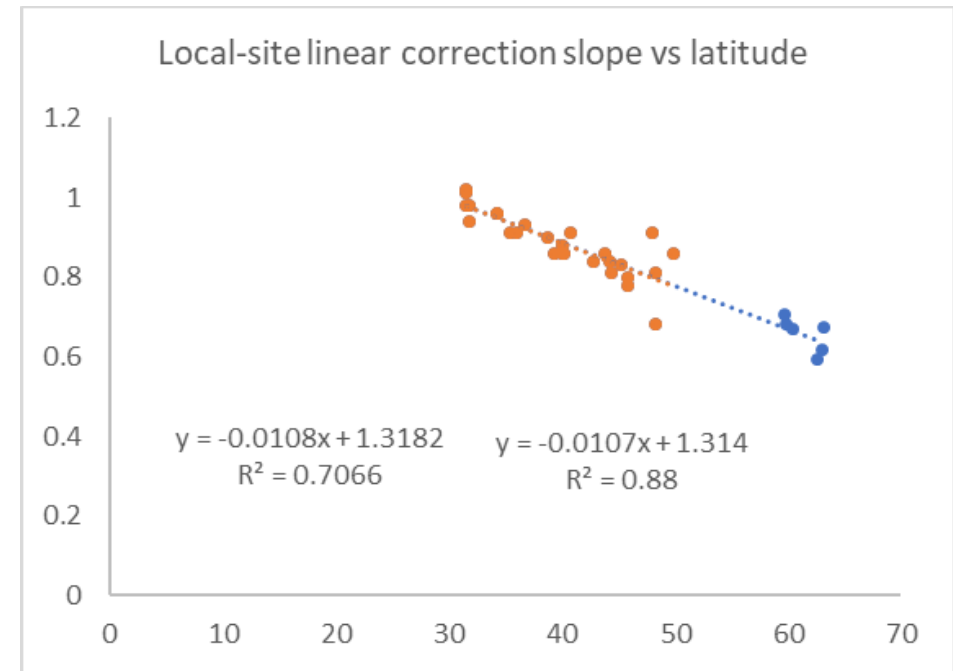
# Families of clear-sky longwave rad models



# Empirical correction model

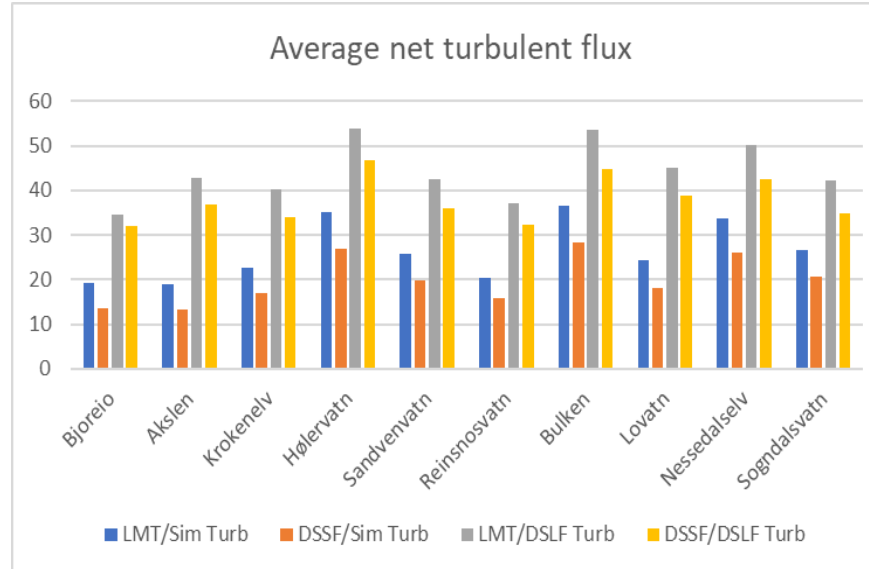
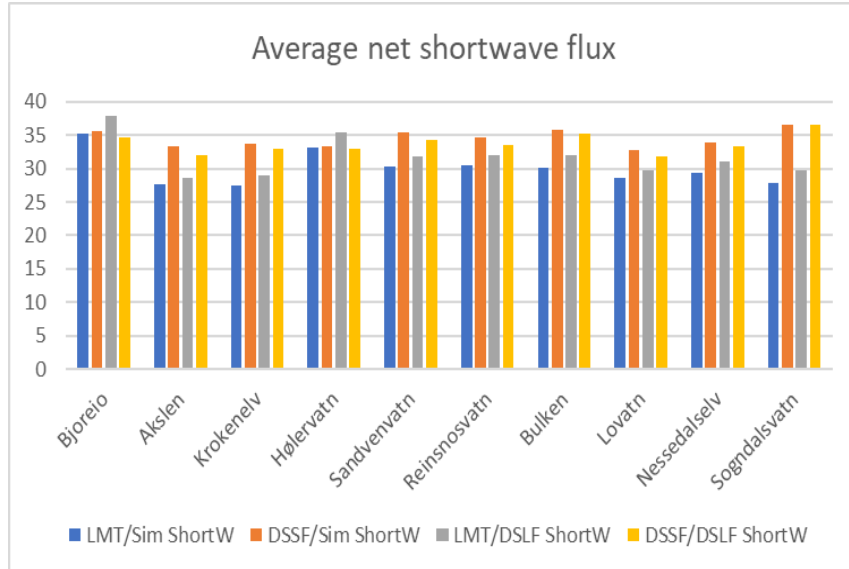
Site	Brunt Method					Brutsaert Method				
	Bias	SD	<i>R</i>	<i>S</i>	<i>I</i>	Bias	SD	<i>R</i>	<i>S</i>	<i>I</i>
Bondville	-0.1	11.8	0.98	0.96	12.1	1.5	14.3	0.98	0.88	36.5
Boulder	17.9	14.7	0.96	0.94	1.5	13.0	14.7	0.97	0.86	30.0
Desert Rock	14.8	8.3	0.98	1.00	-13.8	6.6	8.3	0.99	0.93	17.0
Fort Peck	4.3	15.7	0.97	0.88	30.5	1.7	18.5	0.97	0.81	54.3
Goodwin Creek	-0.1	10.1	0.99	1.05	-17.1	3.2	11.0	0.98	0.96	10.2
Penn State	-2.7	10.9	0.98	1.00	3.4	-2.6	12.6	0.98	0.91	33.6
Sioux Falls	1.8	14.1	0.98	0.94	18.3	2.0	17.2	0.97	0.86	44.5
Bukit Soeharto	-7.3	10.0	0.28	0.25	334.5	-1.6	9.6	0.32	0.3	312.5
Fujiyoshida Forest	2.7	10.3	0.97	0.99	1.8	4.8	11.8	0.96	0.91	27.5
Laoshan	-3.1	11.5	0.99	0.93	22.7	-9.6	17.2	0.99	0.83	55.5
Mae Klong	-9.7	7.0	0.95	1.02	3.5	-3.6	6.7	0.95	1.04	-13.8
Palangkaraya	-5.9	9.3	0.47	0.64	158.0	0.6	9.4	0.44	0.66	144.9
Sakaerat	-13	8.9	0.91	0.95	33.8	-6.7	8.8	0.91	0.96	21.8
Tomakomai	-3.3	10.0	0.98	0.92	28.4	-4.7	12.9	0.98	0.84	52.7
Howard Springs	6.4	13.5	0.90	0.97	5.8	12.8	14.0	0.89	0.91	23.4
Ghanzi grass	16.8	9.1	0.96	1.33	-142.2	16.5	7.1	0.96	1.1	-56.3
Ghanzi mixed	-0.3	9.4	0.89	0.93	26.3	-4.2	11.5	0.90	0.73	104.1
Campbell River	-9.8	15.9	0.89	0.93	31.8	-8.1	16.8	0.88	0.86	50.4

- Wang and Liang (2009) fitted linear corrections to 36 stations
- Stations near Equator and above 500 m a.s.l disregarded
- Published coefficients plotted against latitude (red dots)
- A strong relation was found for both Brunt and Brutsaert models
- Data from 6 Norwegian sites (blue dots) confirms this dependency

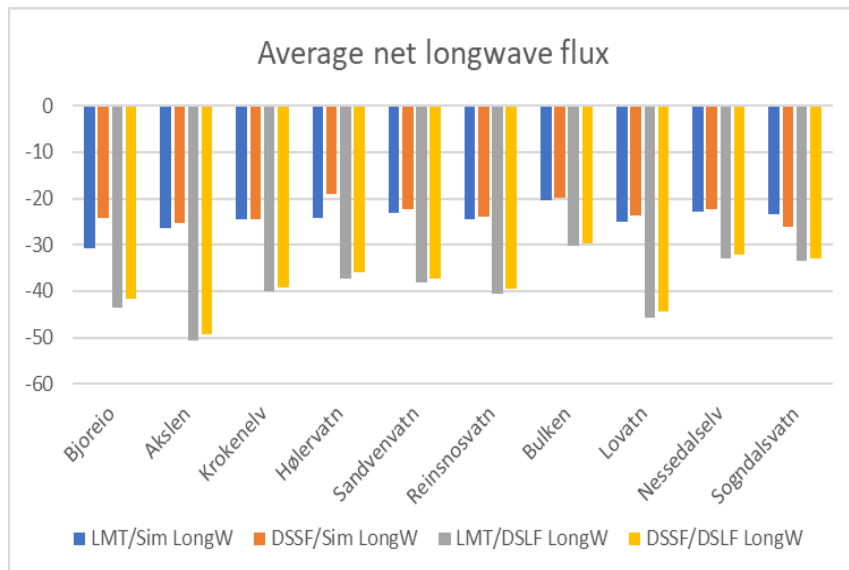




# Snowmelt model evaluation, four cases



- Ground SW, Sim LW
- SEVIRI SW, Sim LW
- Ground SW, SEVIRI LW
- SEVIRI SW, SEVIRI LW



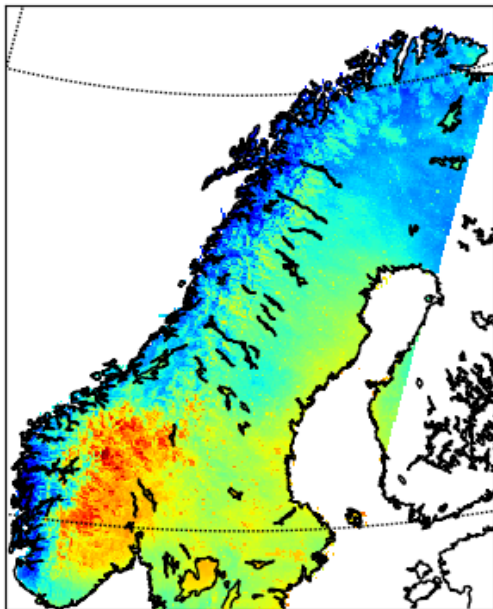
- Small difference between SW data sources.
- Larger differences between LW data sources
- Calibration causes turbulent fluxes to compensate
- Experiment run for 10 catchments, noting average NSE
- The fourth case (SEVIRI SW+LW) improved NSE by approx. 0.02
- Case two and three gave small change in NSE w.r.t base case.

# Evaluation of Arome SW predictions

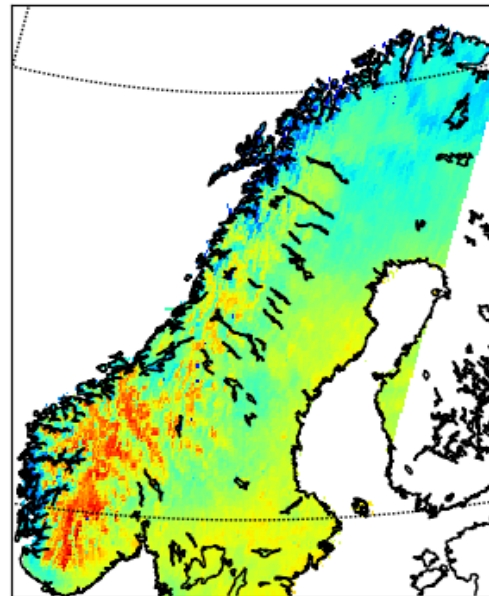
Table and figures:

Åsmund Bakketun, Norw. Met office

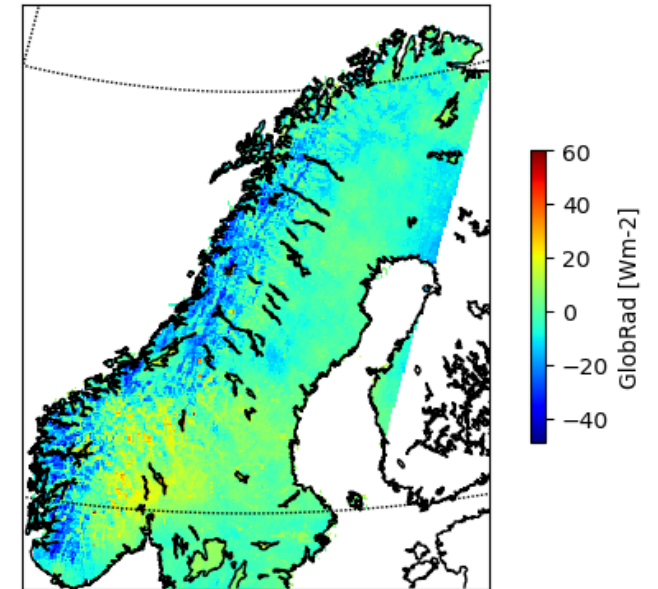
	MEPS / AROME	LandSAF - MDSSF	In Situ
Annual mean [ $\text{W}/\text{m}^2$ ]	99 +/- 10	96 +/- 8	94 +/- 11
Mean abs error [ $\text{W}/\text{m}^2$ ]	Hourly: 35 Daily: 21	Hourly: 29 Daily: 17	-
Correlation CI (clearness index)	Hourly: 0.75 Daily: 0.84	Hourly 0.87 Daily: 0.90	-



MEPS/AROME



LandSAF-MDSSF



Differanse

# Summary

- SW radiation from the local SEVIRI pixel predicts ground measurement as good as a neighbour ground station at 30-70 km distance, varying with latitude and situation
- Models for LW radiation need temperature, humidity, and some clearness index. SEVIRI LW data are cloud-informed model data.
- LW model biases can be compensated using only latitude as extra input
- Using both LW and SW from SEVIRI data in snowmelt modelling, a modest NSE improvement was found.
- Arome predictions of SW radiation show good agreement with both SEVIRI and NIBIO data, with some regional biases.



Thank you for your attention

[Sjur.Kolberg@enki-hydrologi.no](mailto:Sjur.Kolberg@enki-hydrologi.no)